Artificial Intelligence Applications And Innovations Vol. 1 No. 1 (2024)

Article history:
Received 18 August 2023
Revised 17 October 2023
Accepted 21 October 2023
Published online 01 January 2024

A Learning based Compact Wideband mm Wave Antenna Array Design Optimization for 5G iPhone Mobile Handsets

Alireza. Jafarieh[1], Farzaneh. Forouhar[1], Hamid. Behroozi[2], Mahdi. Nouri[3*], Mallat. Nazih Khaddaj[4]

[1] ECE, Sharif University of Technology, Tehran, Iran
[2] Department of Electrical Engineering, Sharif University of Technology, Tehran, Iran
[3] Department of Communication Engineering, Electrical Engineering Faculty, Sharif University of Technology, Tehran, Iran
[4] College of Engineering, Al Ain University, Dubai, UAE

*** Corresponding author email address**: mahdi.nouri@ee.sharif.edu

A r t i c l e I n f o

Article type:
Original Research

How to cite this article:
Jafarieh, A., Farzaneh, F., Behroozi, H., Nouri, M., & Mallat, N.K. (2024). A Learning based Compact Wideband mmWave Antenna Array Design Optimization for 5G iPhone Mobile Handsets. Artificial Intelligence Applications and Innovations, *1*(1), 11-27.
https://doi.org/10.61838/jaiai.1.1.2

A B S T R A C T

In this paper, a mmWave antenna is designed and optimized by machine learning to meet 5G requirements. A Surrogate based optimization approach is used to optimize this antenna. The goals of this optimization are antenna gain, bandwidth, and size. The bandwidth of the optimized antenna covers the 27.5 GHz- 38.9 GHz frequency band. This antenna has a wide 3 dB beam width with 90° and 178° beam width in the E-plane and H-plane, respectively. The realized gain of the antenna is 5 dB in 28 GHz frequency. One of the benefits of this antenna is Its compact size. The total dimension of the antenna is 5.4×5.6 mm^2. In addition, an array of this antenna is proposed with 4 elements. The analog beamforming is achieved by means of this array. The 4-element array is simulated in an iPhone package model. Finally, an antenna with a wide beam, wide band, high gain, and small size is achieved within the Ka-band.

Keywords: *5G, mmWave, Ka bands, Beamforming, mobile communication, and machine learning.*

1. Introduction

The fifth generation (5G) of mobile communication introduces a variety of new applications. Some of these applications are the Internet of Things (IoT), Vehicle to Vehicle communication (V2V), and Vehicle to Infrastructure communication (V2I). The vacant frequency band in the sub-6 GHz band is inadequate to satisfy the requirements for these new applications [1, 2]. In addition, with respect to the small size of the 5G devices, this is essential to design compact antennas. The huge vacant frequency band in the mmWave band seems to be a good choice for the 5G application [1]. In addition, the short wavelength of this band causes the small size of the mmWave devices [3-6]. So mmWave band plays an essential role in 5G. But at these frequencies, due to the high absorption of the atmosphere, radio waves suffer a lot of attenuation. To compensate for this weakening, 5G antennas must have high gain.

One of the things that must be observed in designing a 5G antenna is that different countries have different standards. For example, the 5G standard frequencies are different in the United States, Europe, and China. In the United States, the 28GHz, 37GHz, and 39GHz frequencies are recognized by the Federal Communications Commission (FCC) as the 5G standard bands. The 24.25GHz-27.5GHz frequency band has been introduced by the European Telecommunication Standard Institute (ETSI) in Europe as the 5G frequency band. Therefore, a 5G antenna must be able to work in two or more frequency bands. So, broadband antennas play an essential role in 5G [7].

Due to the high absorption of the environment in millimeter frequencies, the need for antennas with high gain is felt more. Also, due to the small wavelength of this band, it is possible to realize array antennas to achieve this high gain with small dimensions [7-9]. In addition to high gain, in the fifth generation of mobile communication, unlike the previous generations, the need for a fan beam radiation pattern in a specific direction is felt. By using antenna arrays, this radiation pattern can be achieved. In fact, by multiplying the array factor in the radiation pattern of the antenna, a thin radiation pattern can be obtained in the plane perpendicular to the array [7]. Also, in the fifth generation of wireless communication systems, we need to serve different users at different angles without physically changing the antenna (changing the location of the antenna). This is achieved by beamforming [9, 10]. Beamforming by means of array antennas has attracted lots of attention in academic papers and industrial projects in the past years.

There are different methods have been presented to optimize problems that cannot be solved by usual methods. Machine learning optimization is one of these methods that has been used in various applications. Optimizing an antenna has many challenges. The large number of design parameters leads to an optimization with a very large input space [11, 12]. Solving such a problem requires a large number of simulations. A very detailed optimization needs full-wave electromagnetic (EM) simulations that impose a large computational cost [13]. The computational volume of traditional optimization methods, such as population-based methods (PSO), is very high due to the need for a large number of complete simulations. On the other hand, without using a large number of full-wave simulations, the optimization also becomes unrealistic in finding the optimal design. Surrogate-based optimization (SBO) is one of the main solutions, which has a lower computational complexity than traditional methods [11, 14]. In SBO, we try to reduce the computational complexity of optimization by shifting the optimization load to simulations with low accuracy [7]. In the field of antenna improvement, these simulations are carefully applied in different ways. For example, in HFSS, this can be achieved by reducing the number of meshes, number of paths, or by increasing δs.

In antenna optimization, the primary goal is usually to reduce the return loss in the desired band [12]. In the second place, goals such as increasing gain, reducing dimensions, increasing radiation efficiency, etc. are followed [11]. One of the most important challenges of optimizing an antenna is the contradictory optimization goals. This means that improvement in one of these goals usually leads to the weakening of other goals [7]. For example, the gain usually decreases with increasing bandwidth and vice versa. Or, usually, with the reduction of the size, the gain also decreases, and with the increase of the dimensions, the gain increases. Therefore, in antenna optimization, we usually seek to find a trade-off between design goals.

1.1. *Related Studies*

In a study, a microstrip antenna for 5G applications is presented. This antenna is built on a Rogers RT/Duroid 5880 substrate. The overall dimensions of this antenna are $11 \times 9\, mm^2$. This antenna has a wide bandwidth. The bandwidth of this antenna includes the 26 GHz-37.9 GHz band. However, the gain of this antenna in this band is 3.3dBi. A linear array with 4 elements is introduced based on this antenna. The bandwidth of this array covers the frequency band of 26 GHz-37.9 GHz. Also, the maximum gain of this array is 10.2 dB. However, this array does not have fan beam [15]. In another research, a MIMO antenna is designed for applications of the fifth generation of telecommunication systems. The dimension of one element of this antenna is $8.5 \times 6\, mm^2$. The bandwidth of this antenna covers the 27.3 GHz-28.9 GHz frequency band. One element of this antenna has a maximum gain of 7.1 dBi. This antenna is built on a Rogers RT/Duroid 5880 substrate with a thickness of 0.787 mm. An 8-element array is introduced in this paper. This array has an 11.2 dBi maximum gain. The bandwidth of this antenna is 1 GHz, which covers the 27.5 GHz-28.5 GHz frequency band. But, the dimensions of this array are very large [2]. In another study, a diecast antenna for 5G applications is presented. This antenna has dimensions of $10 \times 10 \times 1.5\ mm^3$. This antenna has a 6.8 GHz bandwidth, which covers the 24.1 GHz-30.9 GHz band. The maximum gain of this antenna is 8.5 dBi. This antenna has a circular polarization [3]. In another study, a multiband antenna is optimized by SBO optimization methods. This is a multi-objective optimization problem with the goal of increasing gain and increasing its bandwidth. The ensemble learning method has been used as a model builder in this paper [16]. In another paper, the authors have tried to increase the gain and bandwidth of an antenna by using the pipeline sequential design (PLSD) approach [12]. Also, the co-kriging model builder is used for antenna optimization. In this optimization, the goal is to reduce return loss and antenna dimensions. A broadband antenna for frequencies below 12 GHz has been optimized by an optimization method based on Pareto ranking bisection (PRB). The goals of this optimization are increasing the bandwidth and reducing the size of the antenna [15]. Optimization with the aim of increasing the bandwidth on a dual-band antenna has been done in another sutyd [14]. A square antenna is optimized by an adaptive sampling method (LOLA-Voronoi) in other research [10]. This optimization is done with the aim of increasing the bandwidth and gain of the antenna. In this optimization, it has been tried to optimize the material and thickness of the substrate of the antenna. In another article, artificial neural networks are used to find the return loss model of an antenna in terms of optimizing design parameters. In this article, the aim is to reduce the return loss of the antenna in a very large range. The target range in this article is the 2.9 GHz - 21.6 GHz frequency band [17].

1.2. Main contribution

In this paper, an antenna for 5G applications with wide bandwidth and gain is designed. This antenna is optimized by a machine learning method. Then, using this optimal antenna, a 4-element array have been formed. This array antenna has a fan radiation pattern which is very suitable for 5G applications. Also, beamforming has been done using this array and introduced method [18]. This antenna is simulated in HFSS software. Also, its results have been verified using CST software. In addition, to show the capability of the array, this array is tested in an iPhone model. This work is one of the first 5G mmWave papers which includes a verification test on a mobile phone model. An also is one of the first papers which perform an antenna optimization with goals defined for 5G mobile phone applications.

2. Introduction To DDEA-SE

In the rapidly evolving field of machine learning and optimization, algorithms that leverage the strengths of various methodologies often outperform traditional approaches. One such innovative approach is the Data-driven Evolutionary Algorithm using Selective Ensemble (DDEA-SE) [19]. This algorithm synergizes principles from evolutionary computation and ensemble learning, creating a robust framework for solving complex optimization and predictive modeling problems. At its core, DDEA-SE merges the adaptability of evolutionary algorithms (EAs) with the accuracy and robustness of ensemble methods. Evolutionary algorithms are inspired by natural selection and involve mechanisms such as selection, mutation, and crossover to evolve a population of candidate solutions over successive generations. They are particularly effective in exploring complex search spaces, making them suitable for a variety of optimization problems. In contrast, ensemble learning enhances predictive performance by combining multiple models, thereby improving generalization and robustness against overfitting. By integrating these two paradigms, DDEA-SE addresses the limitations of single-model approaches, which can struggle with both data variety and model accuracy.

The DDEA-SE process begins with the initialization of a diverse population of predictive models. These models may vary in their architecture and parameters, promoting diversity that is crucial for effective ensemble learning. Once initialized, each model's performance is evaluated using a validation dataset, with metrics such as accuracy, precision, and recall helping to ascertain their effectiveness.

One of the distinctive features of DDEA-SE is its selective ensemble mechanism. Based on performance evaluations, the algorithm selects the most promising models and constructs an ensemble. This selection process can involve statistical thresholds or criteria that ensure only the best-performing models contribute to the final ensemble. The integration of effective models enhances the overall prediction accuracy and resilience of the resulting ensemble.

After constructing the ensemble, the algorithm employs evolutionary processes to continuously refine and improve the model population. This includes genetic operations like mutation and crossover, which facilitate the exploration of new model configurations. Importantly, DDEA-SE involves an iterative process, allowing adjustments based on evolving data characteristics or performance requirements. The process of the DDEA-SE is summarized in Table 1.

Table 1

A summary of the process of the DDEA-SE.

Step	Description
Initialization	Generate a diverse population of predictive models using evolutionary algorithms. Set parameters for evolution.
Model Evaluation	Evaluate models on a validation set using performance metrics (e.g., accuracy).
Model Selection	Apply selection criteria to choose the best-performing models for the ensemble.
Ensemble Construction	Construct the ensemble by combining selected models using methods like voting or averaging.
Evolutionary Process	Apply genetic operations to create new model generations, maintaining diversity.
Iteration	Iterate through steps 2-5 until a stopping criterion is reached.
Final Output	Output the best-performing model or ensemble for deployment.

3. Introduction to Single Element Structure

Figure 1 shows the geometry of the initial antenna design. This antenna is designed for resonance at 28 GHz frequency. This antenna consists of two sub-layers with materials Arlon AD 260A and Neltec NX9245 with a thickness of 0.05 mm. In total, this antenna has a thickness of 0.1 mm. The overall dimensions of this antenna are equal to $5.4 \times 6.7\ mm^2$. The size of l_3 is set at λ/4 at a frequency of 28 GHz. Figure 1 a) shows the top layer of this antenna. In this figure, the yellow parts represent the copper metal and the gray part represents the Neltec NX9245 substrate. Figure 1 b) shows the bottom layer of this antenna. The green part in this figure represents copper metal. In Figure 1 b) the blue parts represent the Arlon AD 260A substrate. Figure 1 c) shows the feeding and metal connections of this antenna. As it is clear from this figure, the ground in the upper layer is connected to the metal sheets in the other two layers by means of metal connections. This happened for two reasons. First, in the antenna optimization phase, a frequency-independent structure can be achieved by simultaneously adjusting the parameters of these connections and other antenna parameters through machine learning. These structures play an important role in the design of broadband antennas.

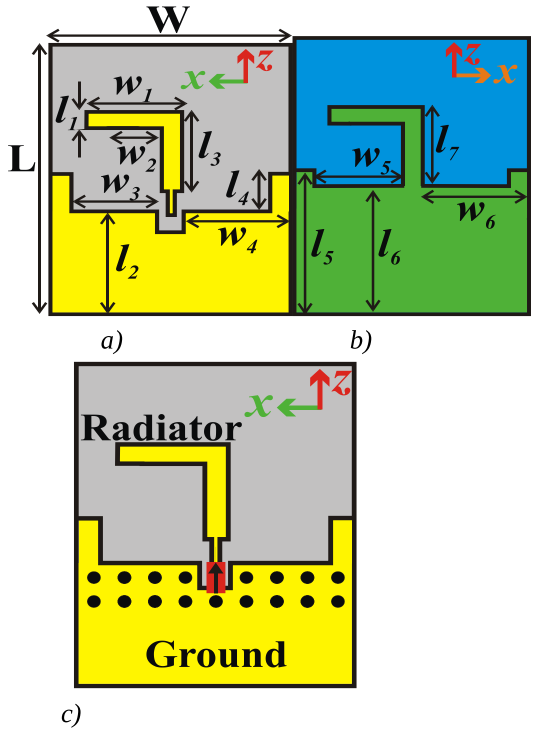

Figure 1

Geometry of the initial antenna: a) Top layer. b) bottom layer. c) metallic vias and antenna port on top layer.

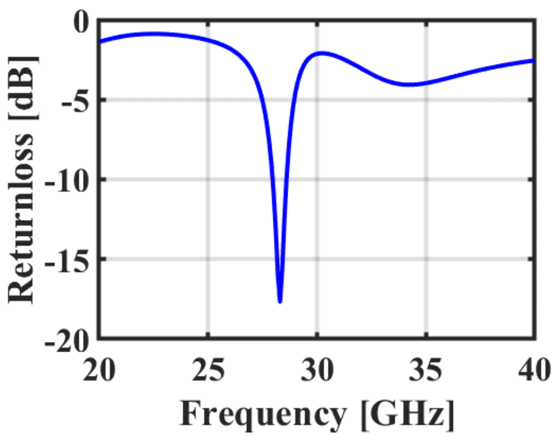

a)

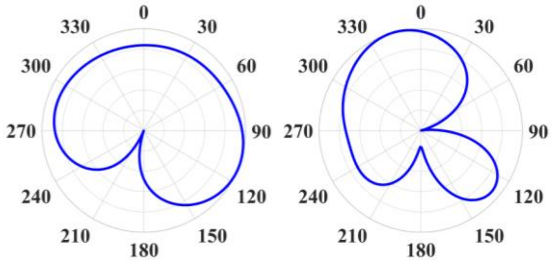

b) *c)*

Figure 2

Outcomes of the initial antenna: a) S-parameter. b) radiation pattern $\phi = 90^\circ$. c) radiation pattern $\phi = 0^\circ$

As a result, an optimal broadband antenna can be achieved by optimizing this structure. The second reason for using this structure is that an antenna array will be designed using this antenna in the following. Due to the short wavelength of the millimeter band and the short distance between the elements of the array, the mutual coupling between the elements of this array will be very large. Considering that the distance between these metal vias is much smaller than the wavelength, these vias can act like the walls of a waveguide and to some extent prevent the leakage of the wave between the ports of the array and keep the wave concentrated in the excitation area. As it is clear from Figure 1, the ground of this antenna is not a complete plane. Because we are looking to design an antenna with a wide radiation pattern. The presence of this ground plane at the bottom of all three layers causes the direction of antenna radiation to be towards its top (positive z direction) rather than towards its back. Figure 2 shows the result of the S parameter of this antenna. This antenna has 700 MHz bandwidth, which covers the 27.9 GHz-28.6 GHz band. The radiation pattern of the first antenna is shown in Figure 2 b), and c). As it is clear from this figure, the radiation pattern of this antenna is very far from the wide pattern we are looking for. In addition, this antenna does not cover the 37GHz frequency band and its bandwidth is very small. Therefore, in order to improve the radiation pattern of the first antenna and improve its bandwidth, it is necessary to make changes to this antenna. Figure 3 shows the modified antenna. The overall dimensions of this antenna are the same as the first antenna. In the second antenna, a tooth has been added to the radiating part of the first antenna, which we have shown in the figure with a length of l_1. In addition, the width of w_1 has also changed in this antenna. The effect of these two recent changes is to increase the bandwidth of the antenna at the resonant frequency of 28 GHz. The sum of these two parameters is set at approximately λ/4 of the 28 GHz frequency. Then, in order to obtain resonance at frequencies close to 35 GHz, another microstrip line has been added to the upper and lower layers. This microstrip line with width of w_7 is shown in Figure 3. In addition to creating resonance near the 35 GHz frequency, this line is also considered as a director. This director is added to the antenna to improve the antenna radiation pattern. Other parameters of the second antenna, including dimensions, substrate, metal vias, and excitation are the same as the first antenna. The values of the first and second antenna parameters are listed in Figure 4

HFSS outcomes of the modified antenna: a) S-parameter. b) radiation pattern $\phi = 90^\circ$. c) radiation pattern $\phi = 0^\circ$

Table 2.

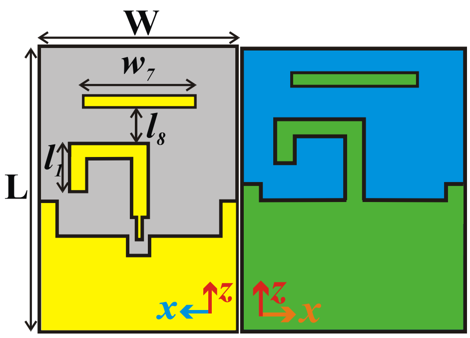

a) b)

Figure 3

Geometry of the modified antenna: a) Top layer. b). (middle layer is same to Figure 1 b))

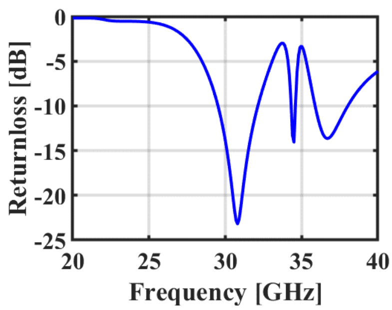

a)

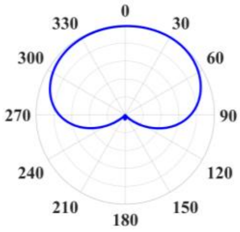

b)

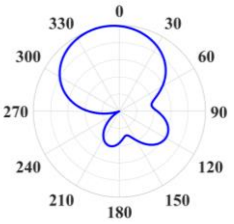

c)

Figure 4

HFSS outcomes of the modified antenna: a) S-parameter. b) radiation pattern $\phi = 90°$. c) radiation pattern $\phi = 0°$

Table 2

Design parameters of the initial antenna.

Param.		L	l_8	l_7	l_6	l_5	l_4	l_3	l_2	l_1
value (mm)	Ant .1	6.7	-	2	3.7	4.4	1.6	2.9	2.6	0.5
value (mm)	Ant .2	6.7	0.3	2	3.7	4.4	1.6	2.9	2.7	0.9
Param.		W	w_8	w_7	w_6	w_5	w_4	w_3	w_2	w_1
value (mm)	Ant .1	5.4	-	-	2.6	2.15	2.5	2.12	1	1.2
value (mm)	Ant .2	5.4	-	2.3	2.6	2.15	2.5	2.12	1	1.6

Figure 4 shows the result of the simulation of the second antenna. As it is clear from this figure, this antenna has two bandwidths. The first bandwidth of the modified antenna has increased in comparison to the first antenna and has reached 2.6 GHz. However, the changes in this antenna have caused a shift in the bandwidth of the first band. Also, these changes have created another bandwidth in frequencies close to 35 GHz. This second bandwidth is equal to 2 GHz.

Figure 4 shows the radiation pattern of the second antenna at 28 GHz frequency. This antenna has a half-power bandwidth of 100° and 186° in $\phi = 0°$ and $\phi = 90°$ planes, respectively. The maximum gain of the antenna at the frequency of 28 GHz is equal to 3.7 dBi.

3.1. Sensitivity analysis

To find the most effective design parameters for the antenna outcomes, Sensitivity analysis is simulated, and the most effective parameters are reported.

Figure 5 a) shows the result of simulating the return loss of the second antenna for different values of l_1. It should be noted that other parameters have the same value as those mentioned in Table 1. As it is clear from this figure, this parameter has a great impact on the return loss of the antenna. In such a way that by increasing this parameter, the first bandwidth of the antenna moves to lower frequencies.

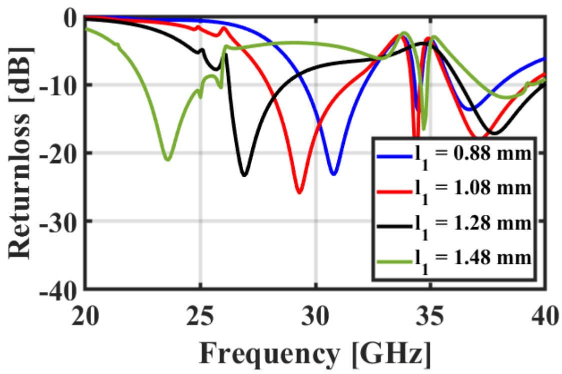

a)

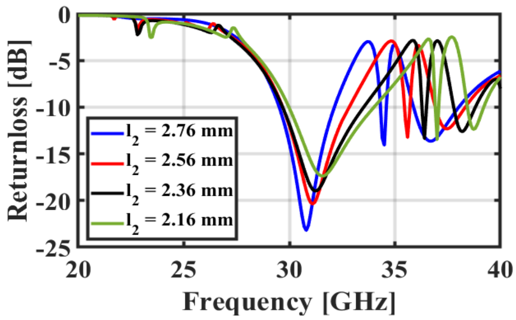

b)

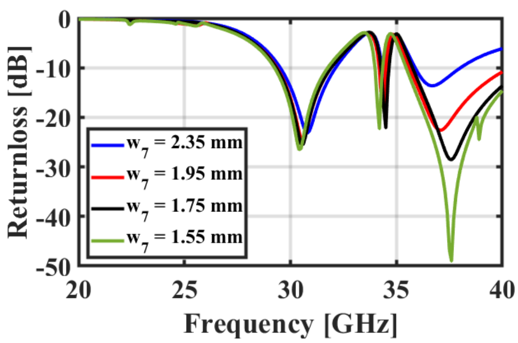

c)

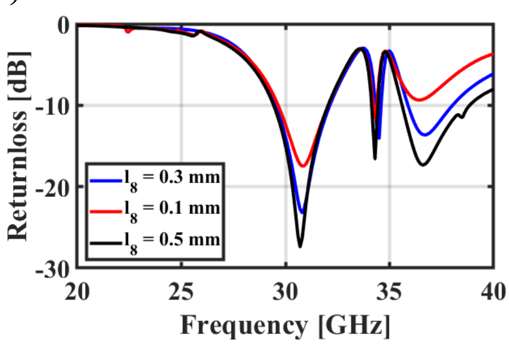

d)

Figure 5

HFSS S-parameter Sensitivity analysis for modified antenna. a) l_1 parameter. b) l_2 parameter. c) w_7 parameter. d) l_8 parameter.

Also, this parameter has a great impact on the value of the second bandwidth. Figure 5 b) shows the simulation results of the return loss of the second antenna for different values of l_2. The effect of this parameter on the value of the first bandwidth of the antenna is evident. Also, changing this parameter has caused the second bandwidth of the antenna to move. The results of antenna return loss simulation for different values of w_7 are shown in Figure 5 c). The effect of this parameter on the first bandwidth of the antenna is very limited and small. But unlike the first band, the second bandwidth of the antenna is strongly affected by the changes in this parameter. By decreasing the value of this parameter, the second bandwidth of the antenna increases greatly. Another parameter related to the director is l_8. It is expected that this parameter, like w_7 , will not have much effect on the results of the first band, but it will have a great effect on the results of the second band. Figure 5 d) shows the effect of this parameter on the return loss of the antenna. As it is shown, the bandwidth of the first band is very little affected by the changes in this parameter. But the second bandwidth shows many changes. So that in one case this bandwidth is completely lost. This observation is completely consistent with our expectations and the logic of our design.

4. Antenna Optimization

In this problem, as in all antenna optimization problems, our first goal is to optimize the antenna parameters in order to improve the return loss of the antenna in our desired band. Due to the different standards of the 5G, we consider the 27.5 GHz-40 GHz frequency band as the desired band to cover most of the mmWave standards. Also, due to the importance of antenna dimensions, the second goal of this optimization is to reduce the antenna dimensions. In order to compensate for the high absorption of the environment in mmWave frequencies, 5G antennas must have a high gain. Therefore, our third goal of this antenna optimization is to increase antenna gain. As a result, we are facing a multi-objective problem.

A very important step in the antenna optimization problem is the selection of optimization parameters. Selecting all the design parameters as optimization parameters requires millions of simulations, and practically the optimization becomes very time-consuming and inefficient. So, it is necessary to select some parameters with the greatest impact as optimization parameters. In the last section, we saw that parameter l_1, l_2, w_7, and l_8 had a significant effect on the results of the primary antenna (Figure 5). It should also be noted that the parameter l_2 has a direct effect on the dimensions of the antenna. Therefore, we choose these parameters as optimization parameters. In addition, due to the importance of metal Vias, we add one of their parameters to the optimization parameters. In this optimization, we consider the distance of these connections from each other as the last optimization parameter.

It should be noted that in this optimization problem, our goals are not definite goals. For example, we would like the return loss to be less than 10 dB throughout the target band. But, for example, modes, where the return loss is 15 dB or 20 dB, are both included in our desirable mode category. And with this calculation, for any mode where the return loss is less than 10 dB, we have an optimal mode. This is also true about the gain and dimensions of the antenna. Considering this issue and considering that different combinations of optimization parameters can create sub-optimal states, this optimization is a non-convex optimization problem. On the other hand, optimization goals are incompatible with each other. For example, the bandwidth usually decreases by increasing the gain. Or by reducing the dimensions of the antenna, its gain also decreases. In fact, in this optimization, we are not looking for the most optimal possible mode, but the goal is to cover the desired band, increase the gain, and reduce the dimensions of the antenna. So, the main goal is to find a trade-off between these goals.

Now we can define the optimization problem mathematically. In the rest of this paper, vectors and matrices are shown in **bold**. The vector of optimization parameters is defined as follows.

$$\boldsymbol{x} = [l_1, l_2, w_7, l_8, d_x] \tag{1}$$

where d_x is the distance between metal vias. Considering that optimization goals are contradictory goals, it is necessary to define the cost function in such a way that this contradiction is controlled as much as possible. Here we are looking for a relationship in terms of gain, return loss and dimensions of the antenna in such a way that the value of this function decreases with increasing gain and decreasing return loss and dimension. It is clear that this function should have a direct relationship with the dimensions and return loss and an inverse relationship with the gain of the antenna. We define the goal vector as follows.

$$\chi = \begin{pmatrix} \widetilde{S_{11}}(\boldsymbol{x}) \\ G(\boldsymbol{x}) \\ A(\boldsymbol{x}) \end{pmatrix} \quad (2)$$

where $\widetilde{S_{11}}(\boldsymbol{x})$ is the average return loss in the desired band in dB unit. $G(\boldsymbol{x})$ and $A(\boldsymbol{x})$ are respectively the maximum gain at 28 GHz frequency with dBi unit and antenna dimension with mm^2 unit. Note that the argument of all three targets is the vector **x**. Antenna dimension is obtained from $A(\boldsymbol{x}) = W \times (3.97 + l_2)$. From now on, we will express these values with $\chi(i), i = 1,2,3,$ where $i = 1, i = 2,$ and $i = 3$ represent respectively $\widetilde{S_{11}}(\boldsymbol{x})$, $G(\boldsymbol{x})$ and $A(\boldsymbol{x})$. Now the cost function can be defined as follows.

$$f(\chi) = \chi(1) + 10 * \chi^{-1}(2) + \chi(3) \quad (3)$$

It is clear that by decreasing the return loss and the area of the antenna and increasing the gain of the antenna, the value of $f(\chi)$ decreases. Note that $\chi(1)$ is a negative value. The factor 10 is multiplied by $\chi^{-1}(2)$ because $G(\boldsymbol{x})$ is a value greater than 1 dBi, and the value of $\chi^{-1}(2)$ in comparison with $\chi(3)$ and $\chi(1)$ becomes very small. If there is no factor of 10, the effect of antenna gain in optimization becomes very insignificant. By defining the cost function in this way, the problem can be changed from a multi-objective problem to a single-objective problem. Now, the optimizer seeks to minimize the function $f(\chi)$. Now the optimization problem can be defined as follows.

$$f^{opt} = \min_{x^{opt}}(f(\chi)) \quad (4)$$

f^{opt} is the optimal (minimum) value of the cost function. $\boldsymbol{x}^{opt}$ is the optimal parameter value vector. The indices of this vector are the optimal values of the optimization parameters that minimize the cost function introduced in equation (3). We display this vector as follows.

$$\boldsymbol{x}^{opt} = [l_1^{opt}, l_2^{opt}, w_7^{opt}, l_8^{opt}, d_x^{opt}] \quad (5)$$

Using evolutionary sampling methods, problem (4) can be solved and the $\boldsymbol{x}^{opt}$ vector can be obtained [19]. But, one of the challenges of antenna optimization is the lack of a mathematical relationship based on the cost function and design parameters. Therefore, before sampling, it is necessary to first solve a regression problem by a model builder in order to obtain the mathematical relationship of the cost function based on the design parameters. Figure 6 shows the block diagram of the optimization process. The optimization procedure starts with a number of low-fidelity (LF) electromagnetic simulations. These simulations have lower computational complexity than usual ones. However, their accuracy is lower than high-fidelity ones. But they are still reliable. Then based on these simulations a database will be achieved. The components of the $\boldsymbol{x}$ are its inputs and f is their corresponding output. Then, to overcome the lack of a mathematical explanation of f based on $\boldsymbol{x}$, this database will be given to a model builder (regressor). The output of the model builder is considered as the cost function for an iterative sample selector (Evolutionary algorithm). The output of this iterative sample selector is $\boldsymbol{x}^{opt}$. The use of the model based on the LF simulations instead of full wave high-fidelity electromagnetic simulations is called surrogate-based optimization (SBO).

Eventually, to verify the performance of the optimizer, we used the HFSS and CST softwares. The so-called data-driven evolutionary algorithm based on selective ensemble (DDEA-SE) is used as the model builder and iterative sample selector. Details about this optimizer are discussed [19].

4.1. HFSS verification

The optimal values of the optimization parameters are as follows. It should be noted that the dimensions are in millimeters.

$$\boldsymbol{x}^{opt} = [1.2, 1.6, 2.4, 0.3, 0.5] \quad (6)$$

Figure7 a) and b) shows the simulation results of return loss and VSWR of the optimized antenna in comparison to the outcomes of the initial antenna in HFSS software, respectively. The optimized antenna has a return loss of less than 10 dB in the 27.5 GHz-38.9 GHz band. This antenna can cover 28 GHz and 38 GHz bands.

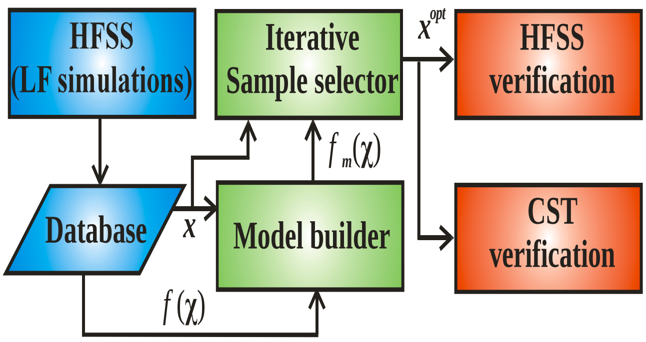

Figure 6

Block diagram of the optimization procedure. LF refers to low fidelity simulations.

As discussed in the last section, the primary antenna does not cover the 28 GHz band and has a small bandwidth in the 38 GHz band. The optimization process has greatly improved the bandwidth characteristics of the antenna. The VSWR of the optimized antenna is less than 1.7 in all working bands of the antenna. Also, this value is less than 1.5 in the 28 GHz-30.7 GHz and34 GHz-37.6 GHz bands. The optimized antenna gain for different frequencies is shown in Figure 8 a). The maximum gain of this antenna at the frequency of 28 GHz is equal to 5 dBi. Also, at the frequency of 38 GHz, the maximum gain of this antenna is equal to 4.7 dBi. The radiation pattern of this antenna at 28 GHz and 38 GHz frequencies is shown in Figure 8 b) and c). The half-power beam width of this antenna at the frequency of 28 GHz in the $\phi = 0°$ and $\phi = 90°$ planes is equal to 80° and 173°, respectively. These values at 38 GHz frequency are equal to 97° and 194° respectively. The direction of the main lobe in the $\phi = 0°$ plane at the frequencies of 28 GHz and 38 GHz is equal to $-5°$ and $-1°$ respectively. Also, this value in $\phi = 90°$ plane for frequencies of 28 GHz and 38 GHz is equal to 19° and 3° respectively

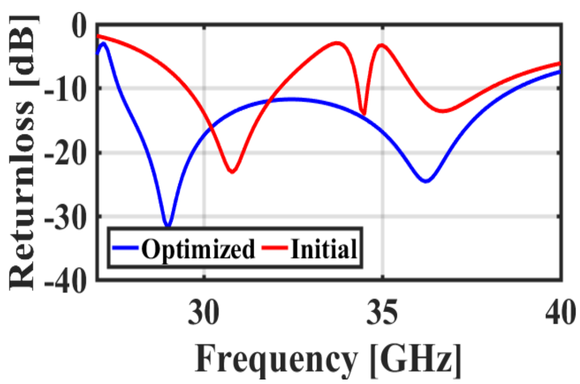

a)

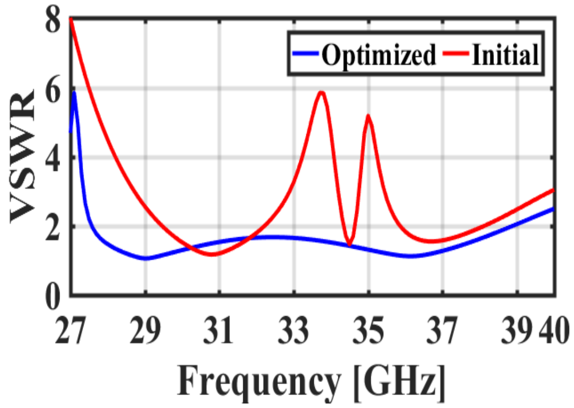

b)

Figure 7

a) S-parameter of the initial antenna and optimized antenna. b) VSWR of the initial antenna and optimized antenna.

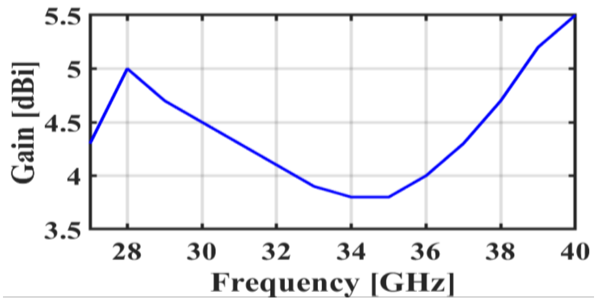

a)

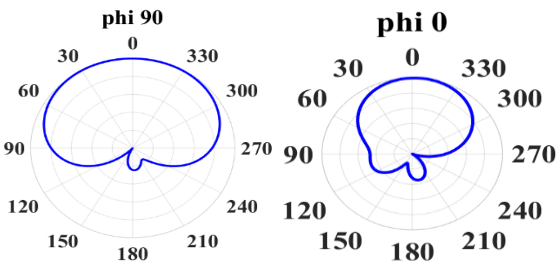

b)

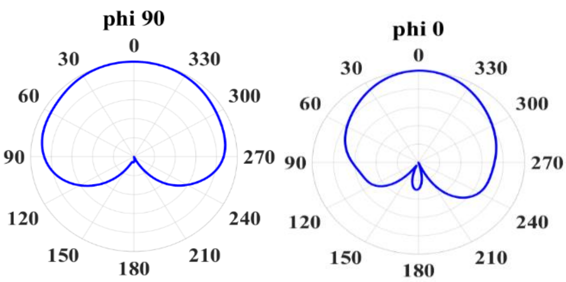

c)

Figure 8

Radiation parameters of the optimized antenna (HFSS). a) Gain versus frequency. b) Radiation patten at 28 GHz frequency. c) Radiation patten at 38 GHz frequency. (ϕ=90^∘ left, ϕ=0^∘ right)

4.2. CST verification

Figure 9 shows the comparison of return loss simulation results in CST and HFSS software. As mentioned earlier, the HFSS results indicate that the optimized antenna in the 27.5 GHz-38.9 GHz band has a return loss of less than -10 dB. The result of the simulation in CST software shows that the optimal antenna in the 28.4 GHz-38.4 GHz band has a return loss of less than 10 dB. The introduced antenna has horizontal polarization. Figure 9

S-parameter comparison between HFSS results and CST.

a) and b) respectively show the antenna radiation pattern in horizontal polarization for $\phi = 0°$, $\phi = 90°$ cuts at 28 GHz frequencies. As it is clear from this figure, the antenna has a half-power beam width of 93.5°in the $\phi = 0°$ plane. Also, the direction of the main lobe of this antenna in this plane is 5°. The maximum gain of this antenna at this frequency is 4.35 dBi. The half-power beam width of this antenna is equal to 166.7° in the $\phi = 90°$ plane. The direction of the main lobe in this plane is 13°. Figure 9

S-parameter comparison between HFSS results and CST.

b) shows the radiation pattern of the optimized antenna at 38 GHz frequency. The half-power beam width of this antenna at this frequency and at the $\phi = 0°$ cut is equal to 78.2°. Also, the direction of the main lobe in this plane is equal to 0°. This antenna has 178.7° half power beamwidth at this frequency and $\phi = 90°$ plane. Also, the direction of its main lobe is 0°. The maximum gain of the optimal antenna in this frequency is 4.69 dBi. The 3D radiation pattern obtained from the CST simulations of this antenna is shown in Figure 11 for 28 GHz and 38 GHz frequencies. At the frequency of 28 GHz, the XPD index of this antenna is 10.2 dB. But at the frequency of 38 GHz, this index is 16 dB.

Table 3

comparison within optimized antenna and state of the art.

Ant.	h (mm)	HPBW (∘)	Max. Gain (dBi)	Relative dimensions	Dimensions (mm^2)	f_{min}-f_{max} (GHz)	f_0 (GHz)
[1]	0.254	- -	3.5	3.27	9 × 11	26-37.9	29
[2]	0.787	- -	7.1	1.68	8.5 × 6	27.3-28.9	28
[4]	0.254	-	6.9	1.98	10 × 6	36.5-37.5	37
[6]	0.787	-	7	2.41	7.7 × 9.5	25-26.2	25.5
[20]	0.508	-	-	2.64	8 × 10	25-31	28.5
[21]	0.254	-	4.5	3.96	20 × 6	25-29.5	27
[22]	0.254	69	5.2	1.48	5 × 9	24.5-33.8	28
[23]	0.76	-	8.1	0.5	3 × 5.4	26.8-29.8	28
[24]	1.57	-	9	52.9	40 × 40	23.8-38.1	30
[25]	0.76	-	9.3	1.23	6 × 6.2	26-30	28
Optimized antenna (CST)	0.11	93.5 (H) 166.7 (E)	4.7	1	5.4 × 5.6	28.4-38.4	28 38
Optimized antenna (HFSS)	0.11	80 (H) 173 (E)	5	1	5.4 × 5.6	27.5-38.9	28 38

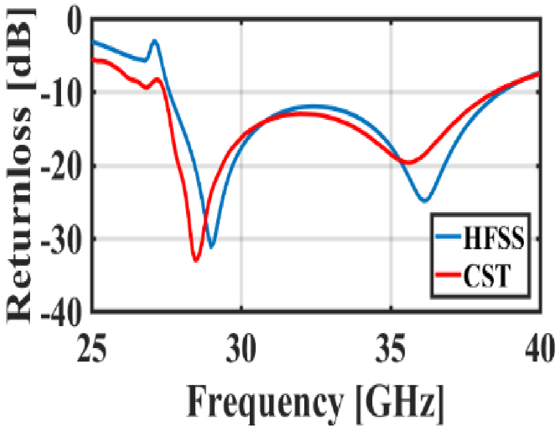

Figure 9

S-parameter comparison between HFSS results and CST.

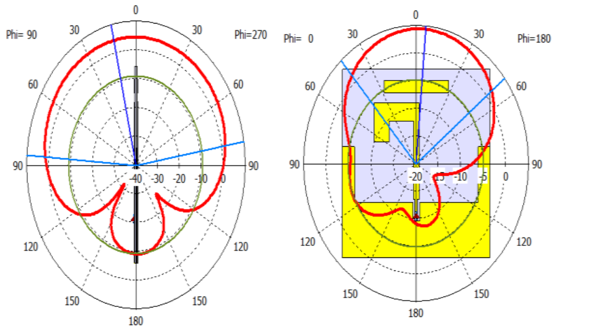

a)

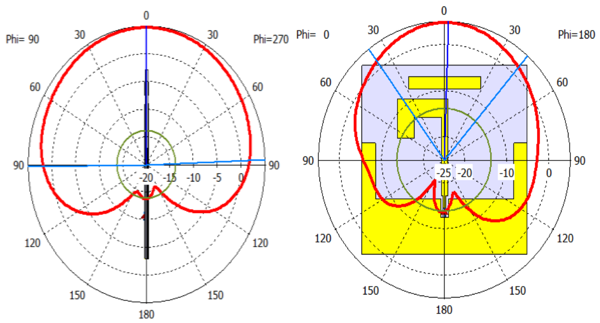

b)

Figure 10

Radiation pattern of the optimized antenna (CST). a) 28 GHz frequency. b) 38 GHz frequency. ($\phi = 90°$ left, $\phi = 0°$ right)

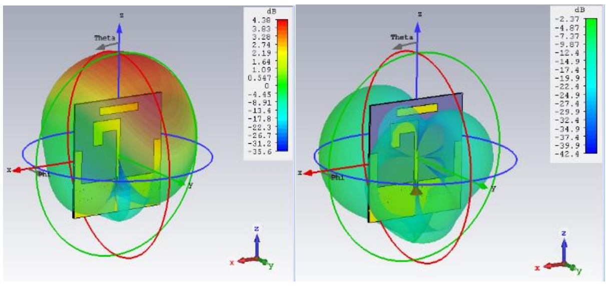

a)

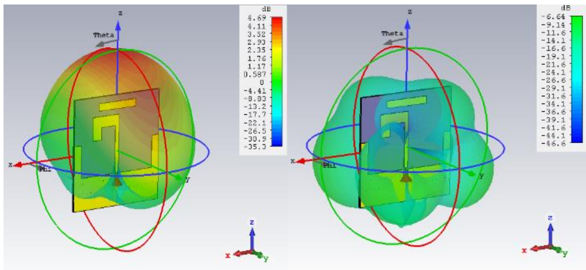

b)

Figure 11

3D radiation pattern of the antenna for horizontal (left) and vertical (right) polarizations (CST). a) 28 GHz frequency. b) 38 GHz frequency.

Table 3 propose a comparison between the proposed antenna and sate of the art. The optimized antenna has smaller dimension than other compared works except Khalid's study [23]. The realized gain of the proposed antenna is larger than some two previous results [1, 21]. The optimized antenna has a larger band width than most of the compared studies except three studies [1, 24, 25].

5. Array Antenna Design

In this section, a 4-element array based on the optimized antenna is proposed. The performance of the antenna is simulated in HFSS and CST. This array is simulated on an iPhone model to show the capability of the proposed array. Figure 12 Shows the geometry of the proposed array antenna. The dimension of the array is equal to $20.4 \times 5.6\ mm^2$. The array elements spacing is equal to half wavelength at the lowest frequency of the operation band.

5.1. HFSS Simulations

Figure 13 demonstrates the S-parameter results of the proposed array. Figure 13 a) shows the return loss result of this array. The bandwidth of this array covers the 27.9 GHz-39.1 GHz band. The result of mutual coupling of the array is shown in Figure 13 b). The mutual coupling between the two side ports of this antenna at 28 GHz frequency is less than 15 dB, and in a large part of its bandwidth, this value is less than 30 dB. The gain per frequency of the array is presented in Figure 14 a). The maximum gain of this array in the pass band is 39 GHz with a value of 10.8 dBi. The maximum gain at 28 GHz and 38 GHz frequencies is 8.8 dBi and 10.5 dBi, respectively. The two-dimensional radiation pattern of an array antenna in the $\boldsymbol{\phi} = \mathbf{90}^{\circ}$ and $\boldsymbol{\phi} = \mathbf{0}^{\circ}$ cuts is shown in Figure 14 b) and c). It should be noted that the normalized radiation pattern is displayed in this figure. This array has an 11 dB sidelobe at $\boldsymbol{\phi} = \mathbf{0}^{\circ}$ and 28 GHz frequency. The half-power beamwidth of this array is $\mathbf{184}^{\circ}$ and $\mathbf{25}^{\circ}$ in $\boldsymbol{\phi} = \mathbf{90}^{\circ}$ and $\boldsymbol{\phi} = \mathbf{0}^{\circ}$ cuts, respectively. Also, the half-power beamwidth of this array at the frequency of 38 GHz at the $\boldsymbol{\phi} = \mathbf{90}^{\circ}$ and $\boldsymbol{\phi} = \mathbf{0}^{\circ}$ cuts are equal to $\mathbf{170}^{\circ}$ and $\mathbf{20}^{\circ}$, respectively.

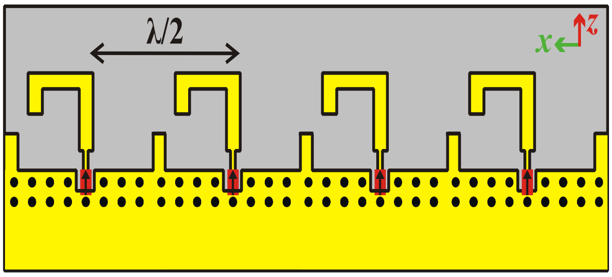

Figure 12

Geometry of the proposed array.

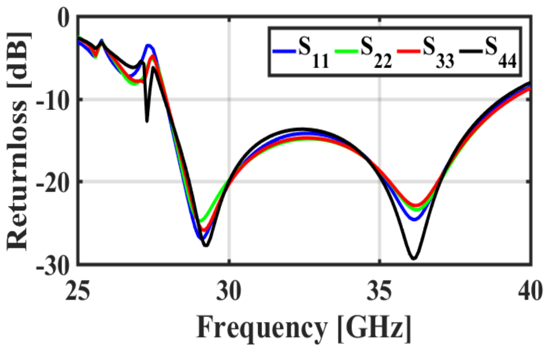

a)

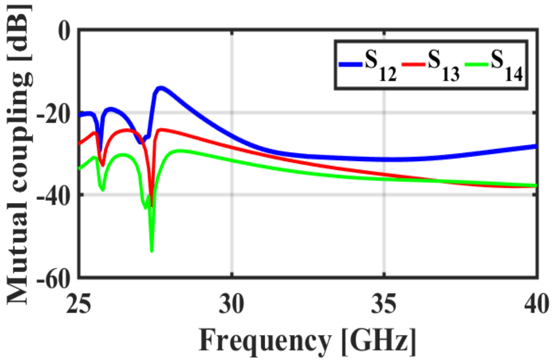

b)

Figure 13

HFSS simulations of the S-parameter of the proposed array. a) Return loss. b) Mutual coupling.

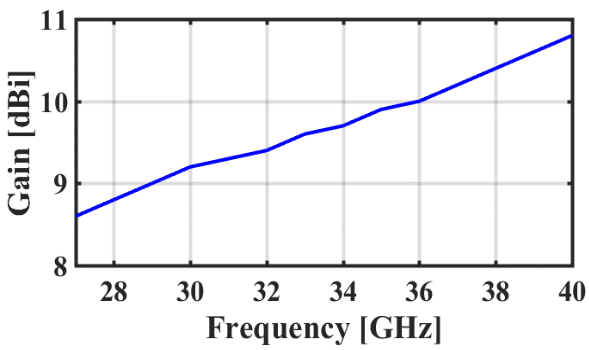

a)

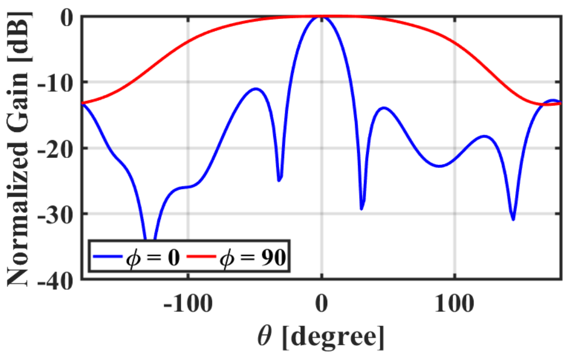

b)

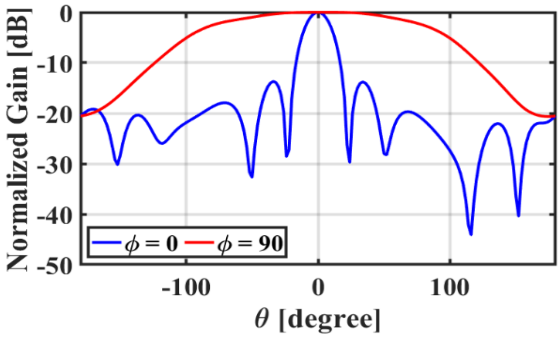

c)

Figure 14

HFSS simulations of the Radiation characteristics of the proposed array. a) Gain vs frequency. b) Radiation pattern at 28 GHz frequency. c) Radiation pattern at 38 GHz frequency.

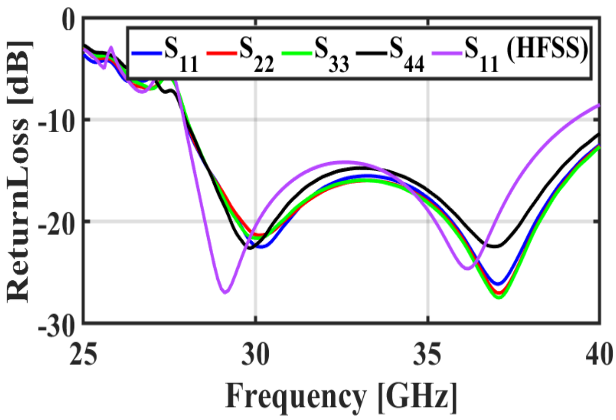

a)

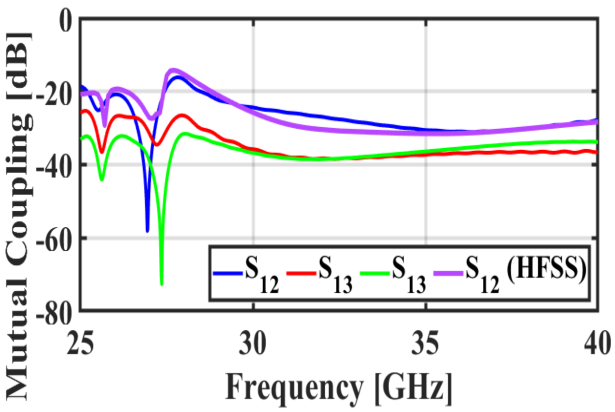

b)

Figure 15

CST simulations of the S-parameter of the proposed array. a) Return loss. b) Mutual coupling.

5.2. *CST Simulations*

Figure. 15 shows the simulation results of the S parameter of this array in CST software. Also, in this figure, the result of the S parameter simulation of the first port in HFSS is displayed for comparison with the CST results. According to these simulations, the array antenna has a 12 GHz bandwidth, which covers the 28GHz-40GHz band. Also, the result of mutual coupling of this antenna array is shown in Figure 15 b). The value of this parameter for two neighbour elements at 28 GHz frequency is equal to 17 dB. This value is greater than 25 dB for a large part of the bandwidth. Figure 16 a) shows the 3D results of the antenna array simulated in CST. This array has 8 dBi and 10.3 dBi gain at 28 GHz and 38 GHz frequencies, respectively. The results of the radiation pattern of this array antenna are shown in Figure 16 b) and c). At 28 GHz frequency this antenna has a half-power beam width of $\mathbf{11.7}^{\circ}$ and $\mathbf{174.3}^{\circ}$ at $\boldsymbol{\phi} = \mathbf{0}^{\circ}$ and $\boldsymbol{\phi} = \mathbf{90}^{\circ}$ cuts, respectively. These values at 38 GHz frequency are equal to $\mathbf{20.1}^{\circ}$ and $\mathbf{169}^{\circ}$.

5.3. *iPhone test*

In order to test one of the applications of this introduced array, we have tried to simulate this antenna in the iPhone 12 model. Figure 12 shows the antenna in the iPhone model. Note that the antenna can be placed in this structure in two ways. One state is when the z axis is perpendicular to the array (called z-normal) and one state is when the x axis is perpendicular to it (called x-normal). The model of this phone is made of aluminum (yellow parts) and polyamide (gray parts).

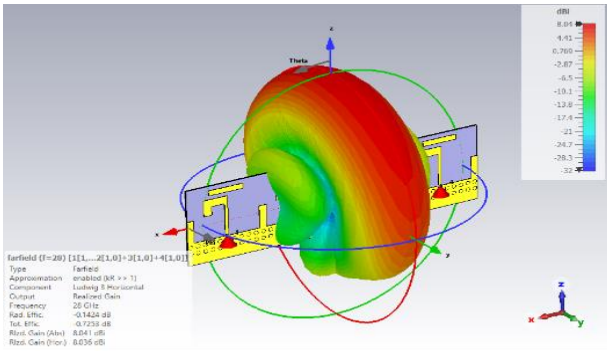

a)

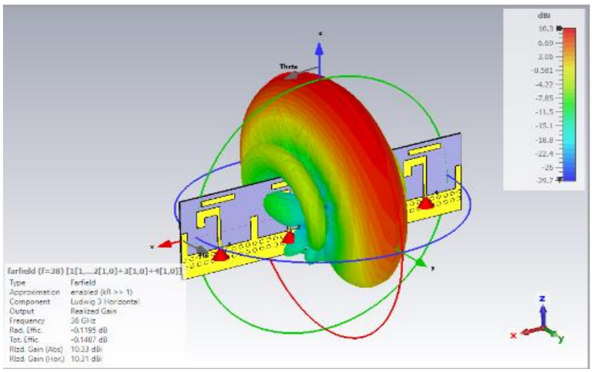

b)

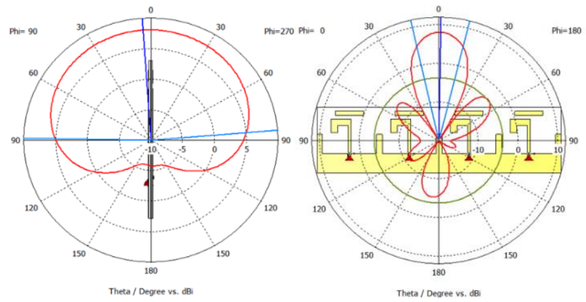

c)

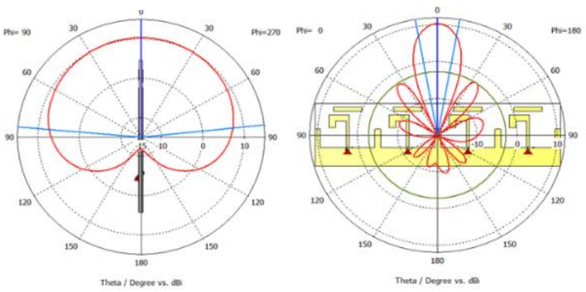

d)

Figure 16

CST simulations of the Radiation characteristics of the proposed array. a) 3D Gain at 28 GHz. b) a) 3D Gain at 38 GHz frequency c) Radiation pattern at 28 GHz frequency. d) Radiation pattern at 38 GHz frequency. (ϕ=90^∘ left, ϕ=0^∘ right)

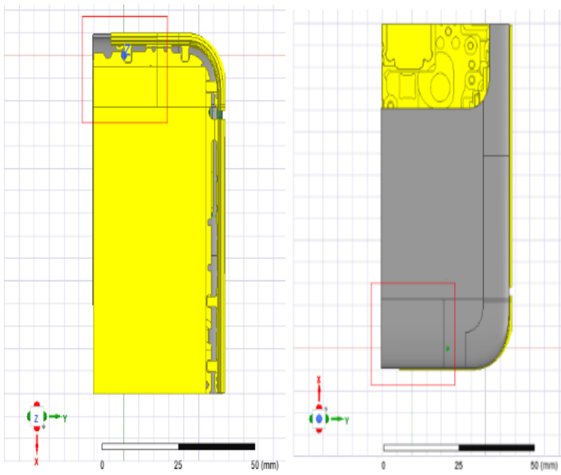

Figure 17

iPhone model for test of the the proposed array.

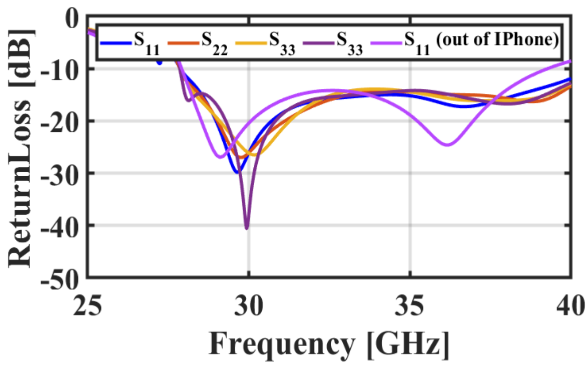

a)

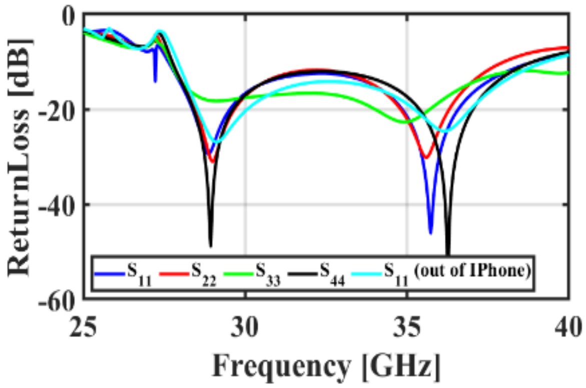

b)

Figure 18

HFSS simulations of the return loss of the proposed array in iPhone model. a) x-normal. b) y-normal.

Figure 18 shows the HFSS simulation results of the S-parameter of these tests. As it is clear from Figure 18, the array bandwidth in the x-normal mode of the array antenna covers the 27.6 GHz - 40 GHz frequency band. Also, the bandwidth of this antenna in z-normal mode covers the 27.6 GHz - 38 GHz frequency band. The radiation pattern and 3D gain of the iPhone test are illustrated in Figure 19. The antenna gain in the x-normal test at 28 GHz and 38 GHz frequencies is equal to 9.62 dBi and 12.44 dBi, respectively.

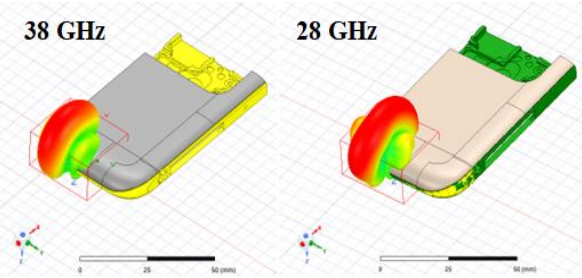

a)

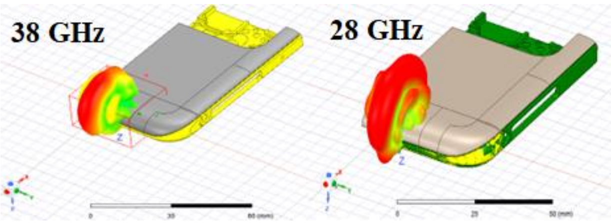

b)

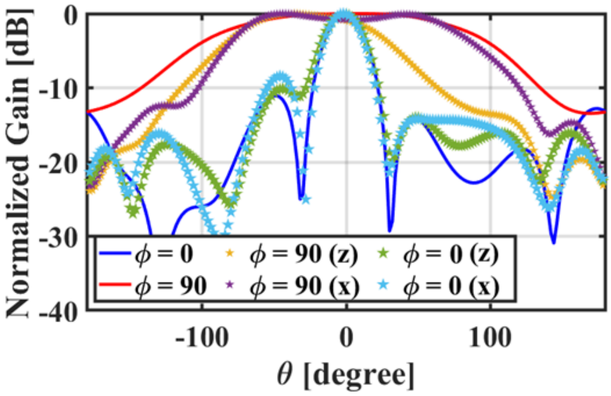

c)

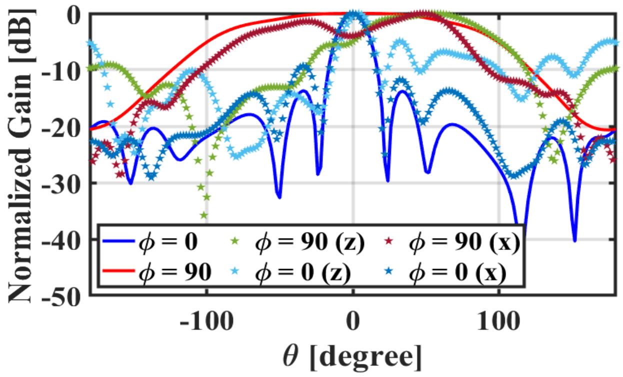

d)

Figure 19

HFSS simulations of the Radiation characteristics of the proposed array in iPhone test. a) 3D Gain (x-normal). b) a) 3D Gain (z-normal). c) Pattern at 28 GHz frequency comparison of z-normal, x-normal, out of iPhone. d) Pattern at 38 GHz frequency comparison of z-normal, x-normal, out of iPhone.

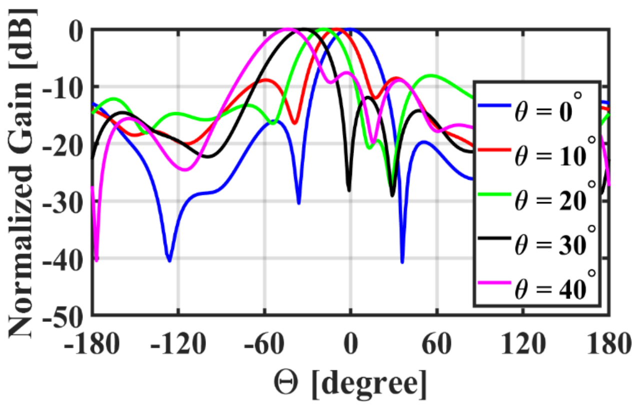

Figure 20

HFSS simulations results of the beamforming test of the proposed array antenna.

At the frequency of 28 GHz, the antenna in the x-normal test has a half-power beam width of 154° and 25° in $\phi = 90°$ and $\phi = 0°$ cuts. These values for 38 GHz frequency are equal to 134° and 19°. In the z-normal test, the gain of the array is equal to 11 dBi and 12.1 dBi in 28 GHz frequency and 38 GHz frequency, respectively. The half power beamwidth at 28 GHz frequency in this test is equal to 102° and 26° in $\phi = 90°$ and $\phi = 0°$ planes, respectively.

The reason for the reduction of the half-power beamwidth in the $\phi = 90°$ cut is the existence of an aluminum plate parallel to the antenna under the antenna, which has reflected a part of the antenna's radiation in the upward direction. In fact, this aluminum plate acts like a reflector. These values for 38 GHz frequency are equal to 82° and 19° in $\phi = 90°$ and $\phi = 0°$ cuts, respectively.

5.4. Beamforming test

In this section, to show the array antenna application on beamforming we have used the beamforming method introduced in Li et al.'s (2017) study [18]. Figure 20 shows the beamforming results of the presented 4-element array antenna. Using the introduced 4-element array and the method introduced in Li et al.'s (2017) work [18], we have been able to change the radiation pattern maximum direction of this array up to $\pm 40°$ angles. Note that the positive angles are not shown in Figure 19, but with a $180°$ phase shift of the array elements, these angles are achievable. With respect to the HPBW of the array beam, this array can cover angles upto $\pm 62°$.

6. Conclusion

In this paper, a mmWave broadband antenna with a wide radiation pattern for 5G applications is proposed. First, an initial antenna for resonance at 28 GHz frequency is presented. This antenna has 700 MHz bandwidth around 28 GHz frequency. Then, with the aim of increasing the bandwidth and beam width, changes have been applied to this antenna. As a result of these changes, the initial bandwidth of this antenna has increased significantly, and another resonance frequency near the frequency of 38 GHz has also been created. In order to increase the bandwidth, gain, and decrease the gain of this antenna, an evolutionary optimization method has been implemented on this antenna. According to the results of HFSS, the optimal antenna has a 10.4 GHz bandwidth, which covers the 27.5-38.9 GHz band. Also, the maximum gain of this antenna is 5 dB and it has a beam width of 80° and 173° in $\phi = 0°$ and $\phi = 90°$ cuts, respectively. The overall dimensions of this antenna are equal to $5.4 \times 5.6\, mm^2$. In addition, a 4-element array of this optimal antenna is presented. The dimension of this array is equal to $20.4 \times 5.6\, mm^2$. Also, its gain at the frequency of 28 GHz is equal to 8.8 dB. This array has a half-power beam width of 25° and 184° in $\phi = 0°$ and $\phi = 90°$ respectively. The 4-elements array has 11.2 GHz bandwidth, which covers the 27.9-39.1 GHz band. In addition, this array is tested in an iPhone model. The beamforming tests done to show the capability of this array.

Authors' Contributions

All authors equally contributed to this study.

Declaration

In order to correct and improve the academic writing of our paper, we have used the language model ChatGPT.

Transparency Statement

Data are available for research purposes upon reasonable request to the corresponding author.

Acknowledgments

We would like to express our gratitude to all individuals helped us to do the project.

Declaration of Interest

The authors report no conflict of interest.

Funding

According to the authors, this article has no financial support.

Ethical Considerations

Not applicable.

References

[1] S. H. Kiani, A. G. Alharbi, S. Khan, M. Marey, H. Mostafa, and M. A. Khan, "Wideband three loop element antenna array for future 5G mmWave devices," *IEEE Access*, vol. 10, pp. 22472-22479, 2022, doi: 10.1109/ACCESS.2022.3152769.

[2] A. Jafarieh, M. Nouri, H. Behroozi, and N. K. Mallat, "A Design of a mmWave Compact Antenna with a Microstrip Line Balun Feed for 5G Communications," in *2022 5th International Conference on Communications, Signal Processing, and their Applications (ICCSPA)*, 2022, pp. 1-4, doi: 10.1109/ICCSPA55860.2022.10019104.

[3] N. K. Mallat, M. Nouri, S. A. Aghdam, M. T. Zia, B. Harb, and A. Jafarieh, "A dual circularly reconfigurable polarization patch antenna for fifth generation mobile communication systems," *Progress In Electromagnetics Research C*, vol. 105, pp. 73-84, 2020, doi: 10.2528/PIERC20053002.

[4] J. Khan, S. Ullah, U. Ali, F. A. Tahir, I. Peter, and L. Matekovits, "Design of a millimeter-wave MIMO antenna array for 5G communication terminals," *Sensors*, vol. 22, no. 7, p. 2768, 2022, doi: 10.3390/s22072768.

[5] M. Nouri, A. Jafarieh, H. Behroozi, N. K. Mallat, M. H. Jamaluddin, and S. A. Aghdam, "Compact 5G millimeter-wave dual-band filter with application in filtenna," *Microwave*

and Optical Technology Letters, vol. 63, no. 2, pp. 620-625, 2021, doi: 10.1002/mop.32637.

[6] S. Tariq, S. I. Naqvi, N. Hussain, and Y. Amin, "A metasurface-based MIMO antenna for 5G millimeter-wave applications," *IEEE Access,* vol. 9, pp. 51805-51817, 2021, doi: 10.1109/ACCESS.2021.3069185.

[7] M. Nouri, H. Behroozi, A. Jafarieh, S. A. Aghdam, M. J. Piran, and N. K. Mallat, "A learning-based dipole yagi-uda antenna and phased array antenna for mmwave precoding and v2v communication in 5g systems," *IEEE Transactions on Vehicular Technology,* vol. 72, no. 3, pp. 2789-2803, 2022, doi: 10.1109/TVT.2022.3217372.

[8] M. Nouri, S. Abazari Aghdam, A. Jafarieh, J. Bagby, and S. Sahebghalam, "A wideband millimeter-wave antenna based on quasi-Yagi antenna with MIMO circular array antenna beamforming for 5G wireless networks," *Microwave and Optical Technology Letters,* vol. 61, no. 7, pp. 1810-1814, 2019, doi: 10.1002/mop.31790.

[9] M. Nouri *et al.*, "A compact filter and dipole antenna with its phased array filtenna and ADMM-BO learning for use-case analog/hybrid beamforming in 5G mmWave communications," *IEEE Access,* vol. 11, pp. 55990-56007, 2023, doi: 10.1109/ACCESS.2023.3276883.

[10] M. Nouri, S. Abazari Aghdam, A. Jafarieh, N. K. Mallat, M. H. Jamaluddin, and M. Dor-Emami, "An optimized small compact rectangular antenna with meta-material based on fast multi-objective optimization for 5G mobile communication," *Journal of Computational Electronics,* vol. 20, pp. 1532-1540, 2021, doi: 10.1007/s10825-021-01723-6.

[11] N. K. Mallat, A. Jafarieh, M. Nouri, and H. Behroozi, "A machine learning based design of mmWave compact array antenna for 5G communications," in *2022 5th International Conference on Communications, Signal Processing, and their Applications (ICCSPA)*, 2022, pp. 1-4, doi: 10.1109/ICCSPA55860.2022.10019147.

[12] A. Jafarieh, M. Nouri, H. Noorollahi, H. Behroozi, and N. K. Mallat, "An Optimized Wearable Textile Antenna Using Surrogate Ensemble Learning for ISM On-Body Communications," *IEEE Transactions on Components, Packaging and Manufacturing Technology,* 2023, doi: 10.1109/TCPMT.2023.3303194.

[13] A. Durmuş and Z. Yıldırım, "Design and Comparative Analysis of E-Shape and H-Shape Microstrip Patch Antenna for IoT Application," *Mühendislik Bilimleri ve Araştırmaları Dergisi,* vol. 6, no. 1, pp. 88-97, 2024, doi: 10.1109/ICEE52715.2021.9544194.

[14] S. Koziel, A. Bekasiewicz, I. Couckuyt, and T. Dhaene, "Efficient multi-objective simulation-driven antenna design using co-kriging," *IEEE Transactions on Antennas and Propagation,* vol. 62, no. 11, pp. 5900-5905, 2014, doi: 10.1109/TAP.2014.2354673.

[15] S. Koziel and A. Pietrenko-Dabrowska, "Robust parameter tuning of antenna structures by means of design specification adaptation," *IEEE Transactions on Antennas and Propagation,* vol. 69, no. 12, pp. 8790-8798, 2021, doi: 10.1109/TAP.2021.3083792.

[16] N. K. Mallat, A. Jafarieh, H. Noorollahi, and M. Nouri, "A novel fractal arrow-shaped mmWave flexible antenna for IoT and 5G communication systems," *Progress In Electromagnetics Research Letters,* vol. 107, pp. 9-17, 2022, doi: 10.2528/PIERL22052405.

[17] M. M. Khan, S. Hossain, P. Mozumdar, S. Akter, and R. H. Ashique, "A review on machine learning and deep learning for various antenna design applications," *Heliyon,* vol. 8, no. 4, 2022, doi: 10.1016/j.heliyon.2022.e09317.

[18] X. Li, Y. Zhu, and P. Xia, "Enhanced analog beamforming for single carrier millimeter wave MIMO systems," *IEEE Transactions on Wireless Communications,* vol. 16, no. 7, pp. 4261-4274, 2017, doi: 10.1109/TWC.2017.2695599.

[19] H. Wang, Y. Jin, C. Sun, and J. Doherty, "Offline data-driven evolutionary optimization using selective surrogate ensembles," *IEEE Transactions on Evolutionary Computation,* vol. 23, no. 2, pp. 203-216, 2018, doi: 10.1109/TEVC.2018.2834881.

[20] M. M. Kamal *et al.*, "A novel hook-shaped antenna operating at 28 GHz for future 5G mmwave applications," *Electronics,* vol. 10, no. 6, p. 673, 2021, doi: 10.3390/electronics10060673.

[21] A. S. Dixit, S. Kumar, S. Urooj, and A. Malibari, "A highly compact antipodal Vivaldi Antenna array for 5G millimeter wave applications," *Sensors,* vol. 21, no. 7, p. 2360, 2021, doi: 10.3390/s21072360.

[22] H. Ullah and F. A. Tahir, "A high gain and wideband narrow-beam antenna for 5G millimeter-wave applications," *IEEE Access,* vol. 8, pp. 29430-29434, 2020, doi: 10.1109/ACCESS.2020.2970753.

[23] M. Khalid, S. Iffat Naqvi, N. Hussain, M. Rahman, M. S. S. Fawad, and Y. Amin, "4-Port MIMO antenna with defected ground structure for 5G millimeter wave applications," *Electronics,* vol. 9, no. 1, p. 71, 2020, doi: 10.3390/electronics9010071.

[24] D. A. Sehrai *et al.*, "A novel high gain wideband MIMO antenna for 5G millimeter wave applications," *Electronics,* vol. 9, no. 6, p. 1031, 2020, doi: 10.3390/electronics9061031.

[25] S. Iffat Naqvi *et al.*, "Integrated LTE and millimeter-wave 5G MIMO antenna system for 4G/5G wireless terminals," *Sensors,* vol. 20, no. 14, p. 3926, 2020, doi: 10.3390/s20143926.